

Near-band-edge optical properties of $\text{GaSe}_x\text{Te}_{1-x}$ mixed crystals

J. Camassel, P. Merle, H. Mathieu, and A. Gousskov

Centre d'Etudes d'Electronique des Solides,* Université des Sciences et Techniques du Languedoc, 34060, Montpellier-Cedex, France

(Received 23 December 1977)

The near-band-edge optical properties of a series of 15 crystals including the two binary compounds GaSe and GaTe have been investigated in great detail at 300, 77, and 1.6°K. The absorption spectra at 77 and 1.6°K show well-resolved excitonic structures and can be classified in two different series. The first one, GaSe-like crystals, corresponds with compositions ranging between $x = 0.7$ and $x = 1$. It is associated with a small interband matrix element for polarization $\vec{E} \perp \vec{C}$ and a large experimental shift of the fundamental edge. The corresponding transition has a predominant anionlike character in good agreement with previous experimental and theoretical finding for the direct gap in the $\text{GaS}_x\text{Se}_{1-x}$ alloy system. The second series of crystals corresponds with compositions ranging between $x = 0$ and $x = 0.35$ (GaTe-like crystals). It is characterized by a much larger interband matrix element and a smaller energy shift. It corresponds with the fundamental absorption edge in GaTe and can be associated with a mixed anion-cation character. A simple analytical model is found which accounts satisfactorily for the change of interband matrix element between GaSe and GaTe. No alloy composition exists in the range: $0.35 < x < 0.7$.

I. INTRODUCTION

The semiconducting III-VI compounds GaS, GaSe, GaTe, and InSe form an interesting class of materials. They crystallize in a two-dimensional layer structure and exhibit rather unusual mechanical properties which are well accounted for by the strong intralayer coupling. However, not all properties exhibit two-dimensional character and many investigations have shown a three-dimensional character of charge carriers in GaSe,¹ and InSe.² The stacking of different layers on top of each other gives rise to different polytypes. With alloying one changes³ (i) the intralayer coupling and (ii) the polytype. Within a layer, the change in bond length and bond energy gives a continuous shift of the band edge versus concentration. The change in polytype gives discontinuities proportional to the strength of the *interlayer* coupling for a given level. For the solid solution $\text{GaS}_x\text{Se}_{1-x}$, which has been the most investigated, discontinuities ranging from³ 400 to^{4,5} 50 meV have been reported depending on the level considered. If one changes now the *intralayer* coupling not slightly, as a function of concentration, but suddenly, as the solid solution undergoes a phase transition, for example, one should observe new discontinuities at least of the same order of magnitude, or even greater, than those induced by the *intralayer* coupling. We have investigated in that way the full series of $\text{GaSe}_x\text{Te}_{1-x}$ mixed crystals.

GaSe has a layer structure shown in Fig. 1(a). It is made of four sheets of selenium-gallium-gallium and selenium atoms, respectively. The two central sheets are connected by a covalent Ga-Ga bond whose direction is always parallel

to the crystal \vec{C} axis. GaTe has also a layer configuration [see Fig. 1(b)] but now 50% of the Ga-Ga bonds run in the plane of the layer. Previous investigations⁶⁻⁸ indicate a definite phase transition from D_{3h} (GaSe-like crystals) to C_2 (GaTe-like crystals) in the concentration range $0.4 < x < 0.74$, but lacked in accuracy to probe the band gap significantly. Raman-scattering

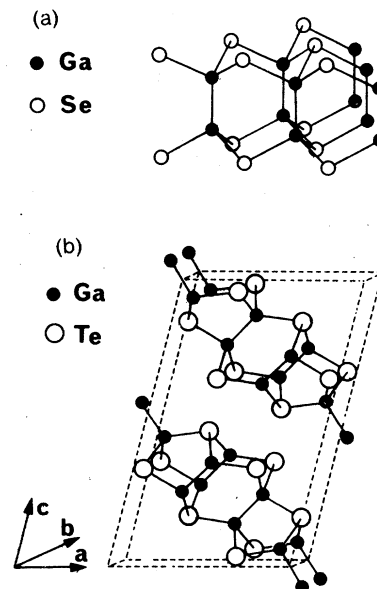


FIG. 1. (a) Perspective view of a single GaSe layer. The Ga-Ga bond direction corresponds with the crystal \vec{C} axis. (b) Perspective view of two GaTe layers extending over one unit cell. The growing direction corresponds with the crystal \vec{b} axis and lies in the plane of the layers. Note the direction of the new gallium-gallium bonds which lie also in the plane of the layer but is perpendicular to \vec{b} .

experiments⁹ also support the structural phase transition.

In this work, we report transmission data obtained at 300, 77, and 1.6 °K under high-resolution conditions. We establish experimentally that the topmost valence band has an identical p_x -like chalcogen character in both GaSe and GaTe. A simple perturbation model is found which accounts satisfactorily for the strength of the fundamental transition (P_1^2) in all III-VI layer compounds.

Next, we investigate the $\text{GaSe}_x\text{Te}_{1-x}$ solid solution. We find two different classes of mixed crystals which is reminiscent of the results obtained in Ref. 3 for the $\text{GaS}_x\text{Se}_{1-x}$ alloy system. The first class corresponds with compositions $0.7 < x \leq 1$. It is associated with a small interband matrix element for polarization $\vec{E} \perp \vec{C}$ (GaSe-like crystals) and a strong experimental shift of the $n=1$ exciton structure versus composition. This corresponds well with the strong anionlike character of the fundamental transition already reported for GaSe.³ The second class corresponds with compositions $0 \leq x < 0.35$. It is associated with a larger interband matrix element for the electric field of the incident light in the plane of the layer and an intermediate shift of the $n=1$ exciton structure versus composition. In the classification of Ref. 3, this corresponds with an intermediate anion-cation character. No alloy composition is found in the range $0.35 < x < 0.7$.

The arrangement of the paper is the following: first, we briefly set the general background of the work. Second, we discuss the experimental procedure. Third, we give our results for the binary compounds GaSe and GaTe. Last, we discuss the two series of mixed crystals.

II. GENERAL BACKGROUND

The layer structure of gallium selenide is shown in Fig. 1(a). This corresponds with a single layer and illustrates the basic properties: strong anisotropy and easy cleaving. Because of stacking considerations, the unit cell of different polytypes extend over two or three different layers and the resulting electronic states have nearly three-dimensional character.^{4, 10}

For GaSe, different band-structure calculations have been reported in the recent years.^{3, 10, 11} They all recognize a strong p_x -like character for the topmost valence bands but it is not clear, at the present time, whether the band originates mainly from selenium,³ gallium,¹⁰ or mixed gallium-selenium states.¹¹ Anyway, because of the p_x -like symmetry, the fundamental transition is allowed only in $\vec{E} \parallel \vec{C}$ polarization. In fact, the

spin-orbit interaction, which mixes on a given atom all p states with different symmetries, contributes to a small admixture of p_x and p_y states and renders the transition slightly allowed in polarization $\vec{E} \perp \vec{C}$. Obviously, the corresponding matrix element should depend on the atomic spin-orbit coupling. It is a goal of this work to investigate the strength of p_x^2 in GaSe and to compare with GaTe. This is done in Sec. IV.

The layer structure of gallium telluride is very different. This is shown in Fig. 1(b), together with the lattice unit cell.¹² The crystal structure is monoclinic (space-symmetry group C_2^2). All layers extend in (102) planes and have their growing direction along the crystal \vec{b} axis. The building units are small blocs (four atoms thick) of tellurium-gallium-gallium and tellurium which (i) extend indefinitely in the \vec{b} direction (growth direction) and (ii) are connected together by new Ga-Ga bonds which lie in the plane of the layer, at right angle with respect to the \vec{b} axis. For near normal incidence conditions, we expect the excitation of the "old" gallium-gallium bond and of the selenium p_x -like states to be forbidden. (Their excitation is restricted to a light polarization \vec{E} "vertical" with respect to the plane of the layer.) Oppositely, we expect the transitions associated with the new gallium-gallium bond to be allowed for a "horizontal" polarization $\vec{E} \perp \vec{b}$ and forbidden when $\vec{E} \parallel \vec{b}$. This has long been recognized and the corresponding transitions have been identified.¹³

At liquid-helium temperature, the fundamental absorption edge appears around 1.79 eV and is allowed in both polarizations $\vec{E} \parallel \vec{b}$ and $\vec{E} \perp \vec{b}$. It is not associated with the new gallium-gallium bond. Indeed, we show in Sec. IV B that the corresponding valence state has a strong tellurium p_x -like character. The excitation of the new bond is found around 2.12 eV: it is allowed for polarizations $\vec{E} \perp \vec{b}$ in the plane of the layer, and forbidden with $\vec{E} \parallel \vec{b}$. As we are interested in this work only with the fundamental absorption edge, we have used near normal incidence and unpolarized light.

III. EXPERIMENTAL PROCEDURE

All samples used in this experiment have been grown from the melt by the Bridgman-Stockbarger technique.⁸ They are in the form of large polycrystalline, cylindrical ingots of which thin samples suitable for transmission experiments are gently cleaved by standard techniques. Their typical dimensions are $2 \times 2 \times 0.02$ mm³. All samples used in the optical experiment have been analyzed with the help of an ionic microprobe

TABLE I. Nominal composition (x^*) and resulting composition (x) obtained from a microprobe analysis for all samples used in the experiment. Also listed are the exciton energy position at 300, 77, and 1.6 °K. (Accuracy ± 2 meV).

Samples	Thickness (microns)	Nominal composition of the melt x^* (at. % selenium)	Sample composition x (at. % selenium)	Exciton peak position (eV)		
				300 °K	77 °K	1.6 °K
GaTe	5.1	0	...	1.667	1.768	1.780
Se (0.1)	5.8	10	9 ± 2	1.700	1.797	1.806
Se (0.3)-2	5.5	30	26.5 ± 1	1.766	1.867	...
Se (0.3)-3	1.3	30	28 ± 2	1.897
Se (0.3)-6	3.8	30	28.5 ± 1.5	...	1.873	1.884
Se (0.5)-5	5	50	32 ± 2	1.797	1.900 ± 0.005	1.905
Se (0.6)	30	60	74.5 ± 1.5	1.886
Se (0.6)-1	22.5	60	73 ± 1.5	1.787	1.870	...
Se (0.7)	...	70	85 ± 1	1.975
Se (0.7)-5	35	70	80.5 ± 1	1.856 ± 0.010
Se (0.8)-2	22	80	87 ± 2	1.890	1.984	1.989
Se (0.85)	29	85	88 ± 1	1.903	1.994	2.003
Se (0.9)-3	36	90	93 ± 1	1.954	2.043	2.050
Se (0.95)	24	95	96 ± 0.5	1.975	2.070	2.077
GaSe	10	100	...	2.001	2.101	2.112

and the resulting compositions are listed in Table I together with the nominal atomic composition of the melt x^* . We find again the general trend previously reported⁸: for $x^* > 0.5$ we have $x > x^*$ and the opposite: $x < x^*$ for $x < 0.5$. No alloy composition is found in the range $0.35 < x < 0.7$ whatever the initial composition of the melt could be. This is in qualitative agreement with the phase diagram for $\text{GaSe}_x\text{Te}_{1-x}$ (Ref. 14) which predicts only alloy compositions in the range $x < 0.1$ and $x > 0.9$.

Our experimental apparatus has been described elsewhere.^{2,15} In this work, the practical resolution of the spectrometer was kept around $1/30000$. The detector was an uncooled S_1 sensitivity-response-curve photomultiplier with standard lock-in amplification techniques. For the low-temperature experiments, we have used a liquid-helium or nitrogen bath Dewar in which the samples, mounted in a strain-free manner, are directly immersed in the cryogenic liquid. During all experiments at liquid-He temperature the fluid was pumped below the λ point. As discussed earlier, unpolarized light and normal incidence were used through all the experiment.

The energy dependence of the transmitted light was carefully checked below the absorption threshold during all transmission experiments. It closely followed the energy dependence of the incident intensity but exhibited multiple internal reflection effects. The sample thickness was deduced from these interference patterns assuming for the refractive index a constant value, independent of the composition. In agreement with the most recent data for ϵ -GaSe,¹⁶ we took the value $n = 2.92$ which accounts for the dispersion

of the refractive index when $\hbar\omega \sim E_g$. It corresponds with photon energies about 0.1 eV below the band gap. The corresponding values at zero frequency for the two binary compounds are, respectively, $n_0 = 2.85$ for GaSe,¹⁶ and $n_0 = 2.70$ for GaTe.¹⁷ The sample thickness obtained are listed in Table I, together with the nominal x^* and resulting x compositions. Also given are the positions of the $n = 1$ exciton peak obtained at 300, 77, and 1.6 °K.

IV. EXPERIMENTAL RESULTS FOR GaSe AND GaTe

A. Gallium selenide

Our experimental results for the best known binary compound GaSe are shown in Fig. 2. The $n = 1$ excitonic structure is well resolved at low temperature and a fairly constant "plateau" is observed at room temperature above the band gap. For sufficiently small values of the broadening parameter,^{2,18} the magnitude of this "plateau" is a characteristic constant of the crystal independent of the experiment. The value found in Fig. 2 is about 1000 cm^{-1} and is in good agreement with previously published data.¹⁶ The strength of the excitonic structure, on the other hand, depends strongly on the temperature, on the crystalline perfection and even, for a given crystal, on the history of the sample (strain, mechanical damage, etc.). We get at 1.6 °K a maximum value of $\alpha \sim 3300 \text{ cm}^{-1}$ which is in good agreement with the results of Ref. 19, but appears rather poor when compared with the work of Ref. 16 ($\alpha_{\text{max}} \sim 6200 \text{ cm}^{-1}$).

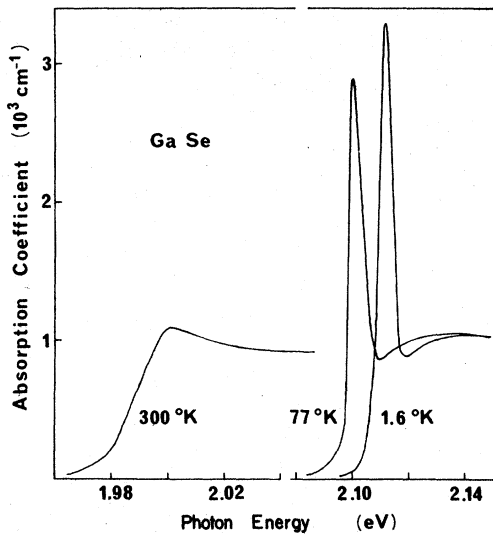


FIG. 2. Absorption spectra obtained at 300, 77, and 1.6 °K for a standard GaSe crystal. Note the magnitude of the $1s$ excitonic peak obtained in this work at 1.6 °K. It compares well, but is not larger, than previously published data.

At low temperature (77 and 1.6 °K) a small bump develops around 2.135 eV in Fig. 2 which is not accounted for by the three-dimensional model of direct excitons.^{2,13} One does not find a similar structure in the nearly perfect three-dimensional layer compound InSe,² and we expect some correlation with the anisotropy of the excitons in GaSe. This point should be discussed at length in a forthcoming publication.

We have estimated the interband matrix element in polarization $\vec{E} \perp \vec{C}$ from the strength of the absorption in the continuum. Indeed, the absorption coefficient for photon energies equal to the band gap writes in practical units^{2,18,20}

$$\alpha_{E_g} (\text{cm}^{-1}) = 9.45 \times 10^{-2} \frac{(\epsilon_{\parallel} \epsilon_{\perp})^{3/2}}{n} R_0^2 f_{cv}, \quad (1)$$

where ϵ_{\parallel} and ϵ_{\perp} are the static dielectric constants, n is the refractive index, R_0 the effective Rydberg energy (in meV) and f_{cv} a dimensionless oscillator strength $f_{cv} = P_1^2 / 2 E_g$.

From the experimental value $\alpha_{E_g} \sim 1000 \text{ cm}^{-1}$, together with $\epsilon_{\parallel} = 6.18$,¹⁶ $\epsilon_{\perp} = 10.6$,¹⁶ $n = 2.92$,¹⁶ $R_0 = 19.5 \text{ meV}$,²¹ and $E_g = 2.13$, we get $P_1^2 = 0.65 \text{ eV}$. This is a very small value in good agreement with the forbidden character of the transition. It must be compared with the recent result² $P_1^2 = 0.6 \text{ eV}$, given for the closely related compound InSe. The main difference between the two crystals is a difference in atomic spin-orbit splitting Δ_0 between the cations.²² If the topmost valence band originated mainly from the cations, for

indium selenide the larger atomic spin-orbit splitting of indium should result in a larger admixture of p_x and p_y with p_z -like states, and in a stronger matrix element. Obviously, this is not the case: within experimental error both results are identical. This demonstrates experimentally the strong anionlike character of the topmost valence band in the III-VI layer compounds GaSe and InSe.

B. Gallium telluride

Typical results for GaTe are shown in Fig. 3. At room temperature, the $n=1$ exciton structure appears at 1.667 eV and is in good agreement with previously published data.^{13,17,23} At low temperature, the broad $n=1$ structure resolves in a very narrow doublet ($n=1; n=2$) which appears both at at 77 and 1.6 °K. We note the strength of the excitonic absorption which is fairly large ($\alpha_{\text{max}} \sim 15500 \text{ cm}^{-1}$ at 1.6 °K) and the small broadening parameter value which is associated with. Obviously, this establishes the excellent crystalline quality of our samples.

There are not much experimental results reported for GaTe and no band-structure calculation. To help identifying the fundamental transition, we have measured (i) the Rydberg energy and (ii) the interband matrix element.

At low temperature the energy positions of the $n=1$ and $n=2$ structures are summarized in Table II. They compare well with other transmission data. The Rydberg energy is deduced from the

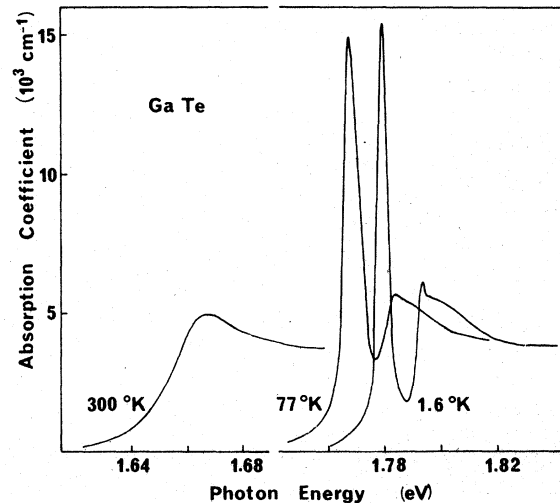


FIG. 3. Absorption spectra obtained for GaTe. Note the nicely resolved doublet at 1.6 °K ($n=1$ and $n=2$) together with the overall strength of the $1s$ structure ($\alpha_{\text{max}} = 15500 \text{ cm}^{-1}$). This constitutes the best results reported up to date and gives an effective Rydberg $R_0 = 19.5 \pm 0.5 \text{ meV}$.

TABLE II. Comparison of the experimental values found for the two first excitonic structures in different works. Within experimental error, the effective Rydberg in GaTe is: $R_0 = 19.5 \pm 0.5$ meV.

Temperatures ($^{\circ}$ K)	1.6	4.2	4.2	77	77	77	77
Reference	a	b	c	a	b	c	d
$E_{n=1}$ (meV)	1779.5	1779 ± 5	1789	1768 ± 0.5	1761 ± 5	1766	1772
$E_{n=2}$ (meV)	1794	1795 ± 5	1806	1784 ± 1	1777 ± 5	1786	1891
$R_0 = \frac{4}{3}(E_2 - E_1)$	19.5	21 ± 10	22	21 ± 1.5	21 ± 10	27	25

^a This work.

^b Reference 23.

^c Reference 13.

^d Reference 17.

two lines $n=1$ and $n=2$ obtained in different works. The best value, from our measurements at 1.6 $^{\circ}$ K, is $R_0 = 19.5 \pm 0.5$ meV. Within experimental error, this is exactly the value reported for GaSe,²¹ which gives a first support to a comparable band scheme.

Let us consider now the interband matrix element. In Fig. 3 the constant plateau for $\hbar\omega > E_g$ is not very well resolved but appears around 4000 cm^{-1} . This is four times the value reported for GaSe. From this value, we estimate the interband matrix element for an unpolarized light in the plane of the layer. With $\epsilon = 7.3$,¹⁷ $n = 2.7$,¹⁷ $R_0 = 19.5$ meV, and $E_g = 1.80$ eV, we get $P_1^2 = 2.8$ eV. This is again a fairly small value. It supports a forbiddenlike scheme for the transition. A qualitative comparison with GaSe and InSe shows a larger interband strength for GaTe which is well accounted for by the larger atomic spin-orbit splitting of Te atoms as compared with Se.²²

A simple model permits a quantitative comparison between all three compounds. We consider only the spin-orbit coupling between the topmost valence band of GaSe (Γ_4^-), which has a strong p_x -like character, and the nearest P_{xy} band (Γ_5^- in the single-group notation). This state constitutes the third valence band^{3,10} and their energy separation $\Delta E = \Gamma_4^- - \Gamma_5^-$ has been well identified.³ It is typically^{3,10,11} ~ 1.5 eV. In first order, we can write the admixture coefficient of Γ_5^- with Γ_4^- ,

$$\frac{2}{3} \Delta_0 / \Delta E, \quad (2)$$

where Δ_0 is the spin-orbit component of the Hamiltonian²²

$$\langle P_{x\uparrow} | H_{so} | P_{x\uparrow} \rangle = \Delta_0 / 3. \quad (3)$$

The interband matrix element in polarization $\vec{E} \perp \vec{C}$ is proportional to the square of the admixture coefficient and writes

$$P_1^2 = \frac{2}{3} P_0^2 \left(\frac{2\Delta_0}{3\Delta E} \right)^2. \quad (4)$$

P_0^2 is an isotropic interband matrix element whose typical value^{24,25} is 20 eV. With the atomic spin-orbit splittings listed in Ref. 22 (0.48 eV for selenium and 1.10 eV for tellurium) together with $\Delta E = 1.5$ eV and $P_0^2 = 20$ eV, we get $P_1^2 = 0.60$, 0.60, and 3.2 eV for GaSe, InSe, and GaTe, respectively. For GaS, the calculation predicts about 0.01 eV.

In Fig. 4 we have plotted the experimental P_1^2 against the estimated value from Eq. (4). The trend is rather satisfactory and supports our crude model. It shows that the topmost valence band, in all three compounds, originates mainly from p_x -like chalcogen levels. This accounts satisfactorily the strength of the "forbidden" transition and shows experimentally that the fundamental direct transition corresponds with an excitation of the p_x -like chalcogen states. This remains true for GaTe and confirms the selection rules previously reported⁴³: the excitation of the new Ga-Ga bond, which lies in the plane

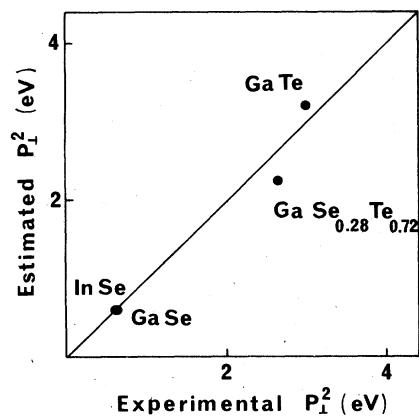


FIG. 4. Comparison of the estimated P_1^2 [Eq. (4)] plotted against the experimental P_1^2 . Note the good overall agreement which demonstrates the strong chalcogen p_x -like character of the top most valence band in all III-VI layer compounds.

of the layer, does not correspond with the fundamental edge but rather with photon energies about 0.3 eV higher. In Sec. V this allows a direct comparison between the two series of crystals.

V. MIXED CRYSTALS

Typical absorption spectra calculated for a series of 13 crystals with nominal compositions, listed in Table I, are shown in Figs. 5-7. For comparison we give also the corresponding spectra for the two binary compounds GaSe and GaTe.

We find at room temperature (Fig. 5) two different series of results. The crystals with compositions in the range $0.7 < x \leq 1$ form a first class of materials with typical absorption strength around 1000 cm^{-1} for photon energies $\hbar\omega > E_g$. They constitute a GaSe-like system with a forbidden direct transition in polarization $\vec{E} \perp \vec{C}$ and a small interband matrix element. The crystals with compositions $0 \leq x < 0.35$ form the second class of materials. They are characterized by an absorption strength which has about four times the value found for the GaSe-like system and correspond with the GaTe crystal structure (monoclinic system). We do not find any intermediate result. This is in good agreement with (i) the prediction of the phase diagram¹⁴ and (ii) the conclusion of earlier studies.⁶⁻⁹

As the temperature is reduced to 77 °K (Fig. 6), the $n=1$ excitonic structure sharpens and

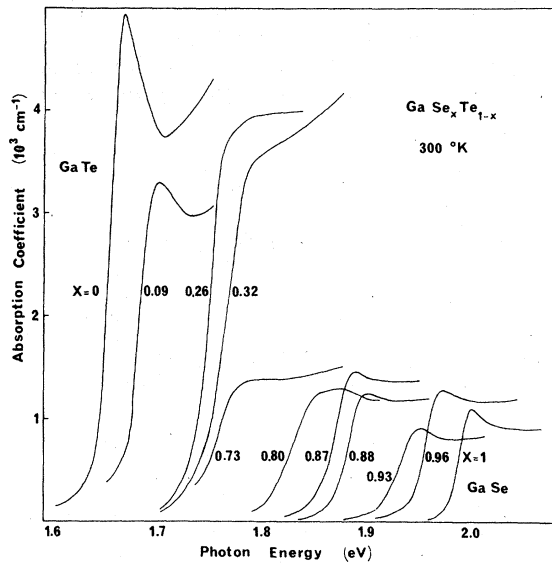


FIG. 5. Room-temperature absorption coefficient obtained for a series of nine mixed crystals. Note the strong difference in absorption strength between all GaTe-like crystals ($x=0.09, 0.26,$ and 0.32) and the GaSe-like one ($x=0.73, 0.80, 0.87, 0.88, 0.93,$ and 0.96).

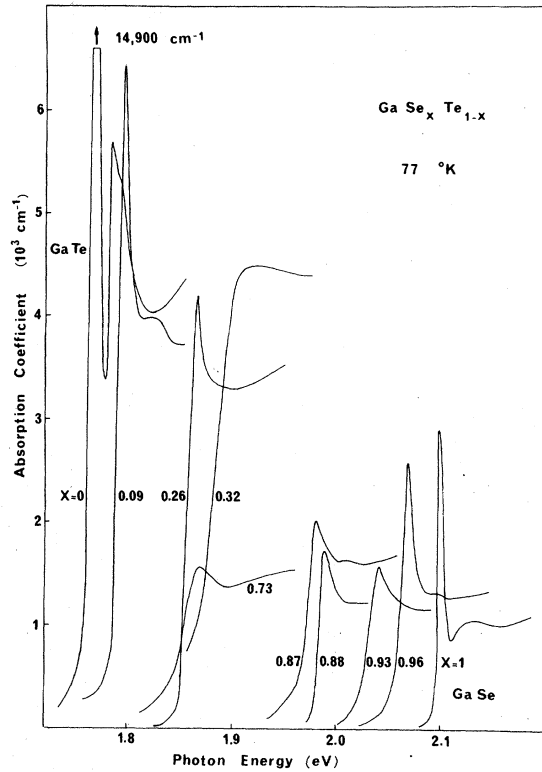


FIG. 6. Same as Fig. 5 but 77 °K.

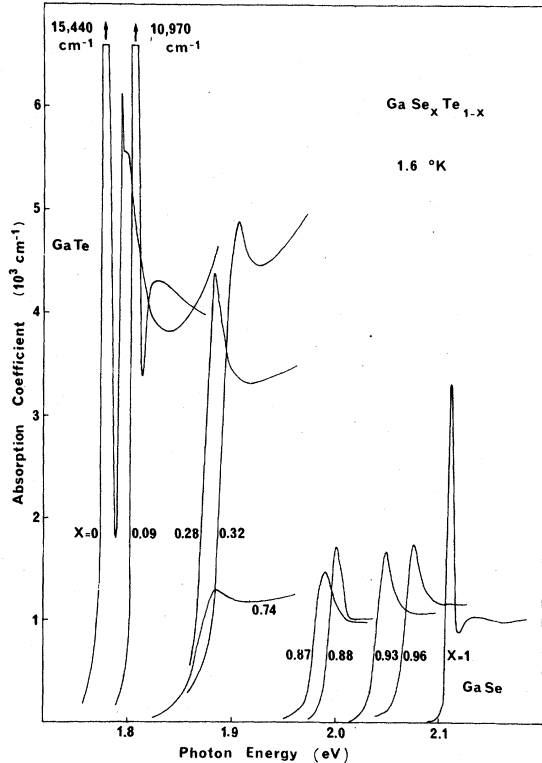


FIG. 7. Same as Fig. 5 but 1.6 °K.

TABLE III. Interband matrix elements P_{\perp}^2 obtained in this work for the series of $\text{GaSe}_x\text{Te}_{1-x}$ mixed crystals. We assume the Rydberg energy ($R_0=19.5$ meV) and the refractive index ($n=2.92$) to be independent of the composition. We take $\langle\epsilon\rangle=7.3$ for the GaTe-like series of mixed crystals and $\langle\epsilon\rangle=8.1$ for the GaSe-like one. The results for composition $x=0.32$ obviously are too high.

x	0	0.09	0.26	0.28	0.32	0.73	0.74	0.87	0.88	0.93	0.96	1
$\langle\epsilon\rangle$	7.3	7.3	7.3	7.3	7.3	8.1	8.1	8.1	8.1	8.1	8.1	8.1
P_{\perp}^2 (77°K) (eV)	3.0	2.8	2.6	...	3.5	0.8	0.7	0.7	0.8	0.65
P_{\perp}^2 (1.6°K) (eV)	2.9	3.0	...	2.65	3.6	...	0.7	0.6	0.65	0.67	0.8	0.65

becomes better resolved. Within a class, the magnitude of the absorption coefficient in the continuum ($\hbar\omega > E_g$) is nearly constant. At pumped liquid-helium temperature (Fig. 7), both the $n=1$ exciton structure and the absorption continuum are clearly resolved for the whole series of crystals. From the magnitude of the continuum, we get the composition dependence of the matrix element for an unpolarized light in the plane of the layer. In agreement with the experimental findings for the two binary compounds, we assume a constant Rydberg energy $R_0=19.5$ meV, a constant refractive index, and the following dielectric constants: $\langle\epsilon\rangle=8.1$ for the GaSe-like crystals¹⁶ and $\langle\epsilon\rangle=7.3$ for the GaTe-like one. The results obtained at 77 and 1.6°K are summarized in Table III. Within experimental error, we do not find a continuous change but rather a two phases picture. This will be discussed in Sec. V A.

The composition dependence of the $n=1$ exciton

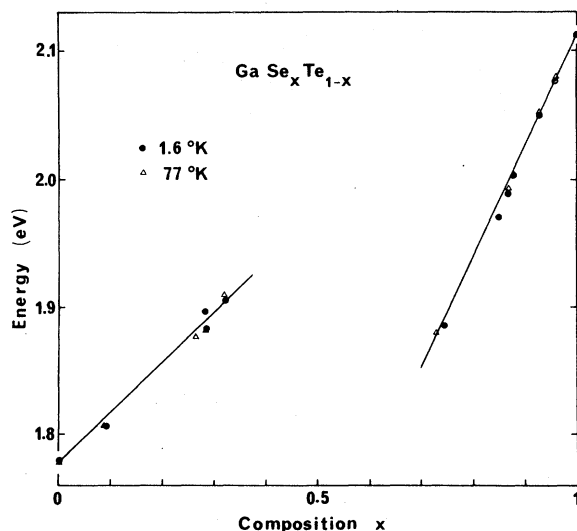


FIG. 8. Composition dependence of the 1s exciton peak in the $\text{GaSe}_x\text{Te}_{1-x}$ alloy system. The results at 77°K have been shifted up by 10 meV for clarity.

peak, as obtained at both 77 and 1.6°K is shown in Fig. 8. (The triangles correspond with the liquid-nitrogen temperature data and have been shifted up for clarity by 10 meV.) The corresponding energy positions are listed in Table I, together with the results at room temperature.

In good agreement with the two-phase picture, we find a straight line of equation $E_{n=1}=2112-870(1-x)$, (meV), for $0.7 < x \leq 1$ which corresponds with the GaSe-like system; and a second line of equation $E_{n=1}=1780+400x$, (meV), for $0 \leq x < 0.35$ which corresponds with the GaTe-like one.

A. GaSe-like systems

The strong experimental shift ($\Delta=870$ meV) is reminiscent of the results already reported for the direct energy gap in $\text{GaS}_x\text{Se}_{1-x}$ alloy system ($\Delta \sim 900$ meV).^{4,5} It corresponds³ with a predominant anion character of the transition and reflects directly the wider separation of occupied p states to empty s states when going from atomic tellurium to selenium and sulfur. Considering only the Γ point of the Brillouin zone, it shows that not only the topmost valence band but also the lowest conduction one have mainly a strong chalcogen character.

The linear composition dependence reported in this work disagrees with the results of previous electroreflectance studies but correlates extremely well with all data³⁻⁵ reported for the $\text{GaS}_x\text{Se}_{1-x}$ solid solution. This is because of our improved experimental conditions and of the systematic use of low temperatures. We cannot directly support the conclusions of Ref. 7 concerning the direct-indirect crossover in $\text{GaSe}_x\text{Te}_{1-x}$ alloys. Indeed,^{2,16} the behavior of the broadening parameter for an excitonic structure is extremely dependent on all external perturbations.²⁶ For perfect binary compounds, for example, it varies from sample to sample and is *not* a characteristic parameter of the crystal. However, we shall get

conclusive informations about the crossover composition. This will be discussed in Sec. V C.

B. GaTe-like system

The composition dependence obtained in this work is $\Delta E = 3.95$ meV/at.%. In qualitative agreement with the results of Refs. 6 and 7, we find a linear behavior but our slope is about 50% higher. Again we believe in the better accuracy of our data. The typical uncertainty in the energy position of the $n=1$ exciton peak is ± 2 meV and the composition is known within $\pm 2\%$.

It is striking to note the close similarity between our slope coefficient ($\Delta = 395$ meV) and the results reported in Ref. 3 for the interband transitions with a mixed anion-cation character ($\Delta = 320-400$ meV). Since the predominant chalcogen p_x -like character of the topmost valence band seems now well established for both GaSe and GaTe, this shows that the conduction band behaves differently in the two series of crystals.

In GaTe, and for the series of mixed crystals with compositions up to $x = 0.35$, the conduction bands originate mainly from empty metal states. The corresponding transition has a strong anion-cation character ($\Delta = 395$ meV) and behaves like the indirect gap in $\text{GaS}_x\text{Se}_{1-x}$ alloys³⁻⁵ ($\Delta = 525$ meV). This is shown in Fig. 9. On the other hand, in GaS, GaSe, $\text{GaS}_x\text{Se}_{1-x}$ alloys and $\text{GaSe}_x\text{Te}_{1-x}$ with composition $0.7 < x < 1$, both the conduction and the valence band have a strong anion character. The band-gap energy shifts almost continuously, independently of the system considered. The average slope is about 9 meV/at.% from GaS to $\text{GaSe}_{0.75}\text{Te}_{0.25}$. This is also shown in Fig. 9.

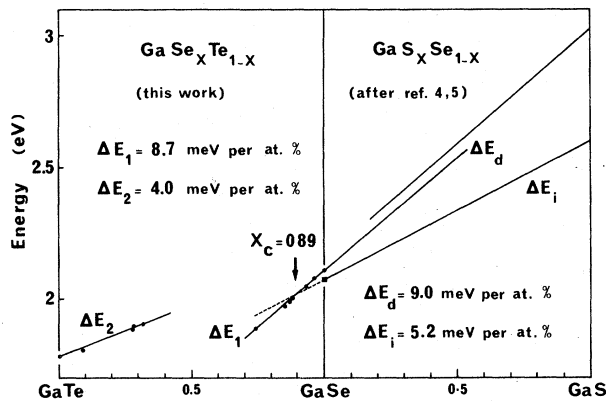


FIG. 9. Composition dependence of the lowest energy gap from GaTe to GaSe and GaS. Note the intermediate energy shift obtained for the indirect transitions in $\text{GaS}_x\text{Se}_{1-x}$ and compare with the direct transition in the GaTe-like series of alloys.

C. Discussion

Since we have established the atomiclike character of all band extrema involved in this alloy system, we can now discuss the direct-indirect crossover composition. First of all, let us remark that there is no good evidence for the indirect gap exciton in most GaSe crystals, even at liquid-helium temperature. Up to date, the corresponding energy position (2.075 eV) is only known from linear extrapolations performed through the whole series of $\text{GaS}_x\text{Se}_{1-x}$ mixed crystals.^{4,5} The slope coefficient is 5.25 meV/at.%. Since the indirect exciton is not resolved in most GaSe crystals by standard optical techniques, it is hopeless to look at it directly in the GaSe-like series of alloys. However, and because of the strong continuity between the two series of crystals (see Fig. 9), we can assume identical slope coefficients. This gives $E_{xi} = 2075 - 525(1-x)$, combining with our result for the direct exciton $E_{xd} = 2112 - 870(1-x)$, we get the direct-indirect crossover at $x = 0.89$. This is shown in Fig. 9.

Coming back to the matrix elements listed in Table III, we can understand now, qualitatively, the nearly constant value found for the GaSe-like series. It results from increased interferences between the direct and indirect transitions. Increasing the tellerium composition, one increases the average spin-orbit splitting²²

$$\Delta_0 = x \Delta_0(\text{Te}) + (1-x) \Delta_0(\text{Se}), \quad (5)$$

and one expects a corresponding increase of the matrix element [see Eq. (4)]. However, as the indirect transition comes closer (see Fig. 9), it becomes resonant and weakens the direct interband matrix element. In good agreement with this qualitative explanation, the lowest value in Table III is reported for $x = 0.87$ which is very close to the crossover composition ($x = 0.89$).

For GaTe-like crystals, one does not expect such interference effects and the trend of P_1^2 versus composition should follow the trend of Eq. (4), with a spin-orbit splitting parameter given by Eq. (5). This is the so-called virtual-crystal approximation. Within experimental error, it works quite satisfactory. Consider the alloy crystal with composition $x = 0.28$. We find in Table III, $P_1^2 = 2.65$ which must be compared with $P_1^2 = 2.25$ obtained from Eqs. (4) and (5). Both results are in fair agreement and follow the trend expected from GaSe to GaTe (see Fig. 4.)

VI. CONCLUSION

We have reported the first investigation of the near-band-gap optical properties of the solid

solution $\text{GaSe}_x\text{Te}_{1-x}$, at low temperature, and under very high-resolution conditions. We have obtained the first experimental evidence of the strong anion p_g -like character of the topmost valence band for the III-VI layer-compounds family. This accounts satisfactory for the strength of the forbidden interband transition obtained in the experiments.

Next, we have investigated the full series of mixed crystals. We have found two different classes of materials. The first one (GaSe-like crystals) corresponds with a strong anion character for the lowest conduction band and a strong energy shift ($\Delta=870$ meV). The second (GaTe-like crystals) corresponds with a cationlike character of the lowest conduction band and an intermediate energy shift ($\Delta=400$ meV). At room temperature we obtain for the band gap energy versus composition $E_g=1.687+0.4x$ (eV), $0 \leq x < 0.35$, $E_g=2.021-0.87(1-x)$ (eV), $0.7 < x \leq 1$. We also obtain the crossover composition between direct and indirect excitonic states in $\text{GaSe}_x\text{Te}_{1-x}$ and we find $x=0.89$.

The large change in lattice structure and bonding between GaSe and GaTe explains the change in atomic character of the conduction band. It

renders rather difficult a direct correlation between the two energy gaps (1.780 eV for GaTe at 1.6 °K and 2.112 eV for GaSe). However, a qualitative examination of the unit cell for both crystals shows a larger extension in real space for GaTe. It suggests a folding down of the first Brillouin zone for GaTe as compared with GaSe. In this case, the lowest conduction band in GaTe would be the "direct analog" of the indirect minimum found in GaSe. Such an effect has already been reported in ZnGeP_2 , the chalcopyrite analog of GaP.²⁷

In qualitative agreement with this simple explanation, we find (i) the mixed anion-cation character of both transitions and the intermediate energy shifts, and (ii) the value 2.067 eV obtained at 1.6 °K from a linear extrapolation of the GaTe-like systems which correlates well the energy of the indirect exciton in GaSe (2.075 eV).

ACKNOWLEDGMENTS

We greatly thank Dr. N. Valignat for the microprobe analysis of our samples. Part of this work was done during a stay at Universidade Estadual de Campinas of A. Gouskov.

*Centre associé au C.N.R.S.

¹G. Ottaviani, C. Canali, F. Nava, P. Schmid, E. Mooser, R. Minder, and I. Zschokke, *Solid State Commun.* **14**, 933 (1974).

²J. Camassel, P. Merle, H. Mathieu, and A. Chevy (unpublished).

³M. Schlüter, J. Camassel, S. Kohn, J. P. Voitchovsky, Y. R. Shen, and M. L. Cohen, *Phys. Rev. B* **13**, 3534 (1976).

⁴E. Aulich, J. L. Brenber, and E. Mosser, *Phys. Status Solidi* **31**, 129 (1969).

⁵C. Depeursinge and Le Chi Thanh, *Proceedings of the Thirteenth International Conference on Physics of Semiconductors*, Rome 1976, p. 388 (unpublished).

⁶E. A. Meneses, N. Januzzi, J. R. Freitas, and A. Gouskov, *Phys. Status Solidi B* **78**, K35 (1976).

⁷V. Lemos, F. Cerdeira, and L. Gourkov, *Solid State Commun.* **20**, 1101 (1976).

⁸L. Gouskov, A. Gouskov, V. Lemos, W. May, and H. Sampaio, *Phys. Status Solidi A* **39**, 65 (1977).

⁹F. Cerdeira, E. A. Meneses, and A. Gouskov, *Phys. Rev. B* **16**, 1648 (1977).

¹⁰M. Schlüter, *Nuovo Cimento B* **13**, 313 (1973).

¹¹J. V. McCanny and R. B. Murray, *J. Phys. C* **10**, 1211 (1977).

¹²W. B. Pearson, *Acta Crystallogr.* **17**, 13 (1964).

¹³N. A. Gasanova and G. A. Akhundov, *Opt. Spektrosk.*

18, 731 (1965).

¹⁴P. G. Rustamov, B. K. Babaev, and M. G. Safarov, *Azerb. Khim. Zh.* **1**, 133 (1964).

¹⁵J. Pascual, J. Camassel, and H. Mathieu, *Phys. Rev.* (to be published).

¹⁶R. Le Toullec, N. Piccioli, M. Mejatty, and M. Balkanski, *Nuovo Cimento B* **38**, 159 (1977).

¹⁷C. Tatsuyama, Y. Watanabe, C. Hamaguchi, and J. Nakai, *J. Phys. Soc. Jpn.* **29**, 150 (1970).

¹⁸R. J. Elliott, *Phys. Rev.* **108**, 1384 (1957).

¹⁹A. Frova, P. Schmid, A. Grisel, and F. Levy, *Solid State Commun.* **23**, 45 (1977).

²⁰D. D. Sell and P. Lawaetz, *Phys. Rev. Lett.* **26**, 311 (1971).

²¹A. Mercier and J. P. Voitchovsky, *Phys. Rev. B* **11**, 2243 (1975).

²²D. J. Chadi, *Phys. Rev. B* **16**, 790 (1977).

²³J. L. Brebner, G. Fisher, and E. Mooser, *J. Phys. Chem. Solids* **23**, 1417 (1962).

²⁴P. Lawaetz, *Phys. Rev. B* **4**, 3460 (1971).

²⁵C. Hermann and G. Weisbuch, *Phys. Rev. B* **15**, 823 (1977).

²⁶J. M. Besson, R. Le Toullec, and M. Piccioli, *Phys. Rev. Lett.* **39**, 671 (1977).

²⁷C. Varea de Alvarez, M. L. Cohen, S. E. Khon, Y. Petroff, and Y. R. Shen, *Phys. Rev. B* **10**, 5175 (1974).